Chapter 5

Speckle-Tracking Imaging, Principles and Clinical Applications: A Review for Clinical Cardiologists

Iacopo Fabiani, Nicola Riccardo Pugliese, Veronica Santini, Lorenzo Conte and Vitantonio Di Bello

Additional information is available at the end of the chapter

http://dx.doi.org/10.5772/64261

Abstract

Evaluation of myocardial mechanics, although complex, has now entered the clinical arena, thanks to the introduction of bedside imaging techniques, such as speckle-tracking echocardiography.

Overcoming the limitations of previous techniques, such as tissue Doppler Imaging (TDI), bi-dimensional (2D) and, only recently, three-dimensional (3D) speckle tracking, allows a fast, reproducible, and semi-automated description of myocardial deformation parameters, including strain, strain rate, velocity, displacement, torsion, and timing of contraction/relaxation. From research tool, speckle tracking has become a great help for clinicians, validated with respect to more complex, time-consuming, and expensive techniques.

Nowadays, further development in technology and image processing draws the attention of the cardiology community. This review intends to describe the fundamental aspects of the imaging technique, together with some recent innovations and clinical applications in this field.

Keywords: cardiac mechanics, deformation, strain, strain rate, speckle tracking

1. Introduction

Speckle-tracking imaging (STI) is a non-invasive ultrasound technique that allows an objective and quantitative evaluation of global and regional myocardial function, independently from the angle of insonation and partly from cardiac translational movements [1–4].

Technique	Advantage	Disadvantage
STI	• Analysis in 2D	• Temporal resolution
	• Tissue movement relative to adjacent segments	• Poor image quality
	• Angle independency	• Myocardial curvature
	• Spatial resolution	• Lower frame rates in tachycardia
	• Low noise	
	• Automated tracking system	
	• Lower interobserver variability	
TDI	• Adequate image quality	• Interobserver variability
	• Temporal resolution	• Time-consuming
		• Technically demanding
		• Low signal-noise ratio
		• Poor spatial resolution
		• Angle dependency
		• One dimension
		• Displacement in relation to transducer

2D, bi-dimensional; STI, speckle-tracking imaging; TDI, tissue Doppler imaging

Table 1. Advantage and disadvantage of different techniques for myocardial deformation analysis.

Echocardiographic estimation of segmental left ventricular contractility is routinely accomplished through visual interpretation of endocardial motion and myocardial thickening. This method is subjective and requires a relatively experienced observer. Quantitative analysis based on tracing of the endocardial border may also be hampered by endocardial "dropout" and trabeculations.

Tissue Doppler imaging (TDI) has been previously used in deriving myocardial velocities and assessing fundamental parameters of myocardial deformation (strain and strain rate) [5]. Myocardial tissue velocities represent the net effect of the contractile and elastic properties of the area under investigation and the motion caused by traction and tethering from other regions. In contrast, strain is a dimensionless index reflecting the total deformation of the ventricular myocardium during a cardiac cycle, as a percentage of its initial length. Strain rate is the rate of deformation or stretch. Strain techniques are, in principle, the optimal modalities for the assessment of regional myocardial function. The major limitation of TDI has been its angle dependency [5], requiring alignment of the ultrasound beam parallel

http://dx.doi.org/10.5772/64261

to the direction of tissue movement. Thus, deformation study was substantially limited to the analysis of the tissue moving toward or away from the probe (**Table 1**).

STI is based on bi-dimensional (2D) echocardiographic technology, not limited by Doppler analysis [6–8]. Segments of myocardial tissue show a pattern of gray values in the ultrasound. This pattern, resulting from the spatial distribution of gray values, is commonly referred to as speckle pattern, characterizes the underlying myocardial tissue acoustically and is unique for each myocardial segment. Speckle tracking allows the measure of all in-plane components of the velocity vector, in all pixels [9]. More recently, the addition of the third dimension (3D) has partly expanded the scope of this technology.

2. Human myocardium

Human myocardium is made up of multiple layers [10–12]. According to the helical model described by Torrent-Guasp, a single myocardial muscle band folding upon itself creates varying orientations of fibers throughout the myocardium, with two principal loops, basal (transverse) and apical (oblique). Myocardium finally consists of three separate layers: transversely oriented circular fibers that wrap (around both ventricles), the inner oblique layer (clockwise rotation), and the outer oblique layer (counterclockwise rotation). Briefly, the myofiber geometry of the LV changes gradually from a right-handed helix in the subendocardium to a left-handed helix in the subepicardium.

The mechanics of the LV is complex, but three principal components contribute to systole: inward motion, longitudinal motion (base moving toward the apex), and differential rotation of the apex and base (twisting). Diastolic mechanics is the opposite of systolic motion. LV torsion (or twist) has an important role in cardiac systo-diastolic mechanics. During the cardiac cycle, there is a systolic twist and an early diastolic untwist around left ventricular long axis, due to opposite apical and basal rotations. Systolic apical rotation is counterclockwise and basal rotation is clockwise [13]. LV rotation is a sensitive indicator of changes in regional and global LV function.

2.1. Cardiac mechanics and limits of conventional indices

Cardiac function is the result of force development (inotropism: opening of the cardiac valves) and deformation (shortening of the myocytes: volume ejection) and can be evaluated globally (pump performance) or regionally [14]. Correct evaluation of systolic function should focus on the intrinsic properties of the fibers and myocytes that represent the real actors behind heart function as well as a pathologic process. The deformation of a myocardial segment during the cardiac cycle is a complex phenomenon and consists of normal deformation (longitudinal shortening/lengthening, radial thickening/thinning, and circumferential shortening/lengthening) and shear deformation (base-apex twisting, epi-endo circumferential shear, and epi-endo longitudinal shear). There is a clear gradient from base to apex in both velocity and displacement (stationary of the apex within the thorax while the base is moving toward it). In contrast, deformation is more or less homogenous throughout the (normal) myocardial wall.

It is important to understand the relation between intrinsic function (contractility) and the resulting motion/deformation. A myocardial segment develops a force but it is also subject to the forces developed by near segments. The intrinsic contractile force of the myocardium (inotropism) is the most important determinant of myocardial performance, but any segment of myocardium is part of a ventricle, with external forces acting up on it (mostly in the opposite direction of the contractile force) and resulting from local wall stress, caused by the intracavitary pressure (related to local geometry of the ventricle) and the interaction with neighboring contracting segments ("pulling" the segment itself). The relationship between acting forces and the resultant deformation is influenced by regional elasticity, which by itself is not a constant; due to the structure of the tissue, the more the myocardium is stretched, the more difficult it becomes to stretch it even further.

Regional myocardial deformation is thus the result of:

Active forces:

- Intrinsic contractility (influenced by tissue perfusion and electrical activation).

Passive forces:

- Intracavitary pressure (afterload/preload; ventricular geometry);
- Segment interaction.

Tissue elasticity:

- Myofibrillar architecture;
- Collagen amount (fibrosis).

Despite this pathophysiological insight, echocardiography is still mainly based on global and indirect indices such as ejection fraction, a volume-based parameter that does not reflect contractility, being based on geometric assumptions. For example, "supranormal" values of ejection fraction (EF) are often found in hypertrophied or volume-overloaded ventricles, thus not reflecting real changes in contractility. EF is also load dependent and, per se, is only a global index, without regional implications and not taking into account segmental interactions, which do not contribute to pump function. Moreover, indices for global functional assessment reflect mainly radial function, ignoring longitudinal function, which is usually altered long before changes occur in radial indices.

2.2. The concept of myocardial deformation

When two neighboring points of the myocardium move at different velocities, myocardium changes its shape (deforming). Otherwise, myocardium is moving but not deforming. When the velocity of the tissue is known, several other parameters can be derived.

Displacement is the integral of the velocity over time (Eq. (1)).

http://dx.doi.org/10.5772/64261

$$d = \int_{T_0}^{T} v(t)dt \tag{1}$$

Strain and strain rate are measures of changes in shape, that is, deformation.

For mono-dimensional deformations, that is, shortening or lengthening, the simplest measurement is conventional or Lagrangian strain (Eq. (2)).

$$\varepsilon(t) = \frac{L(t) - L_0}{L_0} \tag{2}$$

The Greek letter epsilon (ε) is commonly used as a symbol for conventional strain. The strain value is dimensionless and can be presented as a fractional number or as a percentage. For Lagrangian strain, a single reference length (L_0) is defined, against which all subsequent deformation ($L(t)$) will be measured. Strain is positive if L is major than L_0 (an object has lengthened) and negative if L is smaller than L_0 (shortening). If L equals L_0, the strain is thus zero.

Natural strain (ε') is defined as [15]:

$$\varepsilon' = \ln(\frac{L}{L_0}) \tag{3}$$

Natural strain employs a reference length that changes as the object deforms. It therefore describes the instantaneous length change and it is independent of reference times. Compared to that of conventional strain, the natural strain amplitude is smaller for positive strains and larger for negative strains. This concept applies in principle to all three one-dimensional (longitudinal, circumferential, and radial) displacement and strain components.

In two or three dimensions, we should also consider shear strain, i.e., measurement of deformation in angle. It is also mandatory to specify directions and magnitudes of maximal and minimal strain.

The strain rate is the temporal derivative of the strain (Eq. (4)).

$$\varepsilon' = \frac{d\varepsilon}{dt} \tag{4}$$

Whereas strain indicates the amount of deformation, strain rate indicates the rate of the deformation. The spatial gradient in myocardial velocities represents the rate of myocardial deformation, that is, the strain rate. The unit of the strain rate is normally 1/s or s^{-1}. Strain rate is more uniformly distributed along the different regions of the LV, whereas myocardial velocity decreases from base toward apical parts of the LV. Strain can subsequently be derived

by temporal integration of the strain rate curve. Indeed, if the rate of deformation is known at each time instance during the cardiac cycle, the total amount of deformation can easily be calculated. A positive strain rate means that the length of the object is increasing, whereas a negative strain rate means that the length is decreasing. If the length is constant, the strain rate is zero. Therefore, whereas strain is a measurement of deformation relative to a reference state, strain rate is an instantaneous measurement. When the strain rate has been calculated for each time point during the deformation, the strain can be found as the temporal integral of the strain rate (Eq. (5)).

$$\varepsilon' = \int_{T_0}^{T} \varepsilon'(t)dt \tag{5}$$

2D strain comprises four measurements: two natural strains and two shear strains [6].

A 3D model allows the evaluation of three natural strain and six shear strain measurements along x, y, and z or azimuthal axes.

2.3. Fundamentals of speckle tracking

"Speckles" are small groups of myocardial pixels created by the interaction of ultrasonic beams and the myocardium, with specific gray scale characteristics. A speckle is commonly defined as the spatial distribution of gray values in the ultrasound image. The result of a speckle-tracking procedure (followed by regularization process) is an estimate of the in-plane velocity vector in all pixels in each of the frames of the ultrasound data set (dynamic velocity vector field). The spatial distribution of the gray values within the ultrasound image is due to constructive and destructive interference of reflections from the individual scatterers within the myocardium. Reflections occur at transitions between different types of tissues or at specific sites, and are much smaller than the wavelength. Constructive interference generates a high-amplitude signal, destructive a low-amplitude one. The exact scatter positions determine the speckle characteristics. Speckle-tracking technology offers the ability to identify and track the same speckle throughout the cardiac cycle [4].

In the ultrasound image, we see the speckle pattern occurring at a position further away from the transducer. To correctly detect speckles, the motion of the tissue should be slower than the motion of the ultrasound beam (image lines). Sound waves propagate through tissues at an average velocity of 1530 m/s, while myocardial tissue moves at velocities in the order of centimeters per second: the basic condition is thus clearly met [16].

There are different algorithms used by different vendors in tracking these speckles. Some speckle-tracking methods are based on so-called block matching, where a region in the image is selected (the kernel) and is followed in the next image frame by subsequently trying out different positions and by determining the similarity between the kernel and the pattern observed in that position. The position where the similarity between the kernel ("fingerprint") and the observed pattern is maximal is assumed to be the new position of the speckle pattern

http://dx.doi.org/10.5772/64261

[16]. Another common approach is based on conservation of gray value, that is, it is assumed that gray values do not change over time. Radio frequency (RF) speckle—used in block-matching method—is a high-frequency signal, so that small between-frame motion can be detected, whereas its corresponding gray-scale speckle—used in gray-scale tracking—is derived from lower-frequency signals, being less sensitive to small displacements. Importantly, speckle tracking of gray-scale images does not necessarily perform well on high frame-rate data [16]. Then, RF-based methods allow to obtain a higher spatial, temporal, and velocity resolution because they use a signal with a higher-frequency content; at the same time, these methods are more sensitive to decorrelation and noise, requiring more severe regularization, which in turn might limit their resolution. Because both RF and gray-scale approaches offer advantages, a hybrid method was recently proposed.

So far, it is possible to evaluate the direction of movement, the speed of movement, and the distance of such movement at any point in the myocardium, independently from the transducer, relative to adjacent segments. The semi-automated nature of speckle-tracking echocardiography guarantees good intra-observer and inter-observer reproducibility [4].

Given that the velocity vector field is known for all pixels within the image, the axes are known with minimal user interaction. The radial, longitudinal, or circumferential velocity profiles throughout the cardiac cycle can be reconstructed, independent of the angle between the ultrasound image line and the direction of motion as in the conventional Doppler imaging [16]. The process of correcting the initial velocity vector estimates by applying additional boundary conditions based on a priori knowledge about the characteristics of the velocity field is called regularization. Regularization can consist of median filtering, weighted smoothing, elastic model, and myocardial boundaries definition.

Velocity vector imaging is partly analogous to 2D STI as it too tracks the speckles using 2D echocardiography, but utilizes additional physiological information to more robustly track the speckle kernels [17]. Each vector is an expression of direction and the magnitude of the velocity. The qualitative evaluation of the velocity is determined by comparing vectors along the tracked contour. Longitudinal strain is the percentage decrease in the length of the myocardium during systole (movement of the base toward the apex). It is expressed as a percent negative value (decrease in length in systole) [18]. Longitudinal strain may be calculated as an endocardial strain, midline strain, epicardial strain, or averaged over the entire cardiac wall. There is currently insufficient evidence to favor one way over another. Radial strain refers to the thickening of the myocardial wall during inward motion of the ventricle, measured in the short-axis views. The value is traditionally defined as percent positive (thickening in systole). Circumferential strain represents the change in the length along the circular perimeter, by definition percent negative in systole. Strain parameters can be individualized for each myocardial segment or can be expressed as global strain (averaging of all segments). Strain rate (evaluated globally or for each segment) represents rate of longitudinal, radial, or circumferential deformation in time. It has a marked systolic negative peak (S) with two positive peak in early (E) and late diastole (A).

Relevant strain values along strain curves are, but are not limited to:

- End-systolic strain: the value at end-systole;
- Peak systolic strain: the peak value during systole;
- Positive peak systolic strain;
- Peak strain: the peak value during the entire heart cycle. The peak strain may coincide with the systolic or end-systolic peak, or may appear after aortic valve closure (AVC) (it may be described as "post-systolic strain") [19].

Modern software allows display of results in bull's eye (polar map) similar to single-photon emission computed tomography (SPECT). This is more familiar to cardiologists as it depicts single myocardial segments with relative values of strain, strain rate, and time to peak strain/strain rate (synchronicity). A more unfamiliar method to display results in a monoplane view is the so-called curved anatomic M-mode (CAMM) which depicts timely variation of single parameters evaluated for a specific segment of interests from base to the apex and from septal to lateral wall. This offers a unique opportunity for timing and recognizing precise phases of a cardiac cycle (relaxation) and for the evaluation of AVC. End-systole coincides with AVC and can be visualized in the parasternal or apical long-axis view or by detecting the closure click on the spectral tracing of the pulsed-wave Doppler of aortic valve flow [19].

Rotation is the measure of the rotational movement of the myocardium in relation to an imaginary long-axis line from apex to base drawn through the middle of LV cavity 4]. Clockwise rotation is defined as negative, while counterclockwise rotation has a positive value. Twist is the algebraic difference in rotation between the apex and the base. Torsion is the twist normalized for the length of the LV cavity (degrees per centimeter). LV rotation or twisting motion has an important role in LV systolic and diastolic function. Normal values for LV rotation and twist angle have shown high variability (technique used, location of the region of interest, age, and loading hemodynamics of the ventricle). The increase in LV twist angle with age observed in literature can be explained by less opposed apical rotation, resulting from a gradual decrease in subendocardial function with aging. Worsening of diastolic relaxation and reduced diastolic suction is, however, associated with an early reduced and delayed diastolic untwisting.

Myocardial strain and Strain Rate (SR) are sensitive parameters for the quantification of diastolic function. Diastolic SR signals can be recorded during isovolumic relaxation, during early filling, and in late diastole. The hemodynamic determinants of protodiastolic strain rate include LV relaxation, regional diastolic stiffness, systolic function, end-systolic wall stress, and filling pressures. In addition, protodiastolic strain rate can assess interstitial fibrosis and can be used to identify viable myocardium after stunning and infarction. Measurement of diastolic strain and strain rate may be useful for research applications but is presently not recommended for routine clinical use.

The detection of myocardial fibrosis and viability depends on the evaluation of myocardial characteristics and shape during the cardiac cycle. Fibrotic tissue may be focal (as occurs in patients with myocardial infarction [MI]) or diffuse (systemic or metabolic disturbances). Fibrosis is actually accurately identified using myocardial late enhancement or T-weighted

http://dx.doi.org/10.5772/64261

mapping with cardiac magnetic resonance imaging (MRI), but speckle tracking (especially systolic and protodiastolic strain rate) has a good correlation with tissue fibrosis, evaluated via cardiac magnetic resonance or biopsy.

All these parameters can be measured not only for the LV but also for the right ventricle (RV) and left and right atria (LA and RA, respectively), but have not been fully validated and, still together, commercial applications to process these chambers do not exist.

Timing peak strain is pivotal in defining dyssynchrony as well as for the evaluation of ischemia (post-systolic thickening or shortening).

2.4. Image acquisition

Gated images are obtained during end-expiratory breath holding with stable electrocardiographic traces, avoiding foreshortening of the ventricle and proper visualization of endocardial border. Images acquired should be of high quality. Optimal frame rate should be 60–110 frames per second (FPS). The operator should keep the sector width and depth minimal to focus on the structure of interest. Usually, three consecutive cardiac cycles are obtained and the values averaged for the final processing. Low FPS limits tracking efficacy, while higher FPS "smooths" speckle pattern and the final quality of the analysis. Apical four-chamber, two-chamber, and three-chamber views are necessary for estimation of LV strain and strain rates by 2D STI. This finally offers global longitudinal strain (GLS) value, that is, the average of longitudinal strain for all segments in all views. Parasternal short-axis views (basal, papillary muscles, and apex) are necessary for radial and circumferential strains (finally averaged in global radial and circumferential strain) and strain rates as well as for rotation, twist, and torsion analysis. The ways myocardial segments are divided widely vary among vendors, but in general, a 16–18-segment LV model is used. Myocardium is divided into six segments: basal septal, mid septal, apical septal, apical lateral, mid lateral, and basal lateral. For the timing determination of cardiac events, mitral inflow and LV outflow velocities are recorded using pulsed-Doppler echocardiography and the aortic and mitral valve closure/opening (AVC/O and MVC/O, respectively) times are obtained, as well as visually (AVC in apical long-axis view) or semi-automatically (evaluation of CAMM). The recordings are analyzed offline using semi-automated computer software for estimation of strain and strain rate by 2D STI. A region of interest (ROI) has to be outlined manually, tracing the endocardium. The epicardium is automatically traced by the system, but the wall thickness can be manually adjusted.

The ROI is defined at end-diastole by [19]:

- Endocardial border;
- Epicardial border;
- Myocardial midline.

Each of these contours can be user defined or generated automatically.

Topographic definitions of the myocardial ROI in apical views are [19]:

- "Left/right base";
- "Midbase";
- "Apex";
- "Left/right ROIs."

Vendors have incorporated tools to help users identify tracking reliability. Various methods are utilized. Some vendors have introduced protocols that identify segments where tracking is suboptimal and is excluded from the final results. In addition, some vendors provide accuracy indices to guide the user in tracking performance estimates.

Longitudinal strain is more robust and reproducible than other parameters. The values tend to be partly different for different walls and segments. There is a gradient of longitudinal strain values from base to apex (higher values for apical segments) as well as from endo to epicardium (higher values of strain in the subendocardial region). **Table 2** depicts the recently published data on normal values for different strains of LV, while **Table 3** depicts the principal advantages and pitfalls of different strain imaging techniques [20].

Longitudinal Strain	**Circumferential Strain**	**Radial Strain**
Apical septal	Anterior	Anterior
21 ± 4	24 ± 6	39 ± 16
Mid septal	Lateral	Lateral
19 ± 4	22 ± 7	37 ± 18
Basal septal	Posterior	Posterior
17 ± 4	21 ± 7	37 ± 17
Apical lateral	Inferior	Inferior
21 ± 7	22 ± 6	37 ± 17
Mid lateral	Septal	Septal
19 ± 6	24 ± 6	37 ± 19
Basal lateral	Anteroseptal	Anterospetal
19 ± 6	26 ± 11	39 ± 15

Table 2. Mean percentage left ventricular strain values for strain in healthy adults.

A recent meta-analysis identified normal values for strain as (GLS) -19.7% (95% CI, −20.4 to −18.9%), global circumferential strain (GCS) −23.3% (95% CI, −24.6 to −22.1%), global radial strain (GRS) 47.3% (95% CI, 43.6–51.0%). Age, gender, body mass index, systolic blood pressure, frame rate, and equipment vendor were considered the variables most likely to influence GLS. In a general linear model, only mean blood pressure was independently associated with higher values of strain. The differences in each strain component are probably actually linked to technical motives: the superiority of longitudinal strain is linked to the

http://dx.doi.org/10.5772/64261

reliability of measurements in the axial plane respective to azimuthal one; the variability of radial strain may reflect the limited amount of tissue to track in the short-axis view of the non-hypertrophied heart; the ROI, which is user defined, may affect the strain amplitude [21]. 2D strain parameters have been validated against tagged MRI studies and sonomicrometry studies [22–24]. 2D strain data correlate well with TDI-derived ones, although with higher strength and reproducibility [2].

	TDI	2D STI	3D STI
Feasibility	++	++	+
Reproducibility	++	++	+++
Temporal resolution (strain curves)	+++	+	–
Spatial resolution (strain curves)	++	+	+
Angle independency	–	+	++
Validation: simulated	+	+	+
Validation: in vitro	+(+)	+(+)	+
Validation: in vivo	++	++	++
Validation: other techniques in clinical scenario	++	+++	+
Defined normal values	+++	+++	–
Time sparing	–	++	++
Standardized software	–	+/-	–

2D, bi-dimensional; 3D, three-dimensional; STI, speckle-tracking imaging; TDI, tissue Doppler imaging.

Table 3. Tissue Doppler imaging, bi-dimensional and three-dimensional speckle-tracking imaging.

2.5. 3D strain

With developments in ultrasound transducer technology and both hardware and software computing, systems capable of acquiring real-time volumetric LV data are now widely available. Reasonable spatial and temporal resolution of 3D data sets can now be achieved. The ability to estimate true 3D myocardial motion and deformation using various STI approaches may provide cardiologists with a better view of regional myocardial mechanics, which may be important for diagnosis, prognosis, and therapy. These 3D approaches can measure all strain components in all LV segments from a single acquisition [25–27]. Furthermore, they are angle independent, do not suffer from strain estimation errors associated with out-of-plane motion, and may in theory allow more precise calculations of LV twist and assessment of shear strain components [28–31]. This tool is promising for the evaluation of deformation parameters, although only preliminary data are available. A single apical full-volume acquisition is performed, according to standard modalities, with an FPS between 18 and 25 (3D temporal resolution is lower than that obtained with 2D images) [32]. This avoids multiple acquisitions making readily and instantaneously available evaluation of strain

parameters and torsion. The operator is able to limit foreshortening and properly identify walls and segments [33, 34]. 3D strain offers a combined assessment of longitudinal and circumferential strain [35]. To evaluate transmural (radial) deformation, due to image quality and tracking limitation, a derivative parameter, area strain, has been introduced. However, it is important to note that full volume is the result of a stitching process, which can limit tracking of speckles. Frame rate and lateral resolution can also limit good tracking.

2.6. Recent advances and consensus: need for standardization

Recognizing the critical need for standardization in strain imaging, in particular in order to derive a common standard for GLS, the most affordable parameter, in 2010, the European Association of Echocardiography and the American Society of Echocardiography (ASE) invited technical representatives from all interested vendors to participate in a concerted effort to reduce intervendor variability of strain measurement [36, 37]. In order to obtain a perfectly defined strain, synthetic ultrasound images simulated from mathematically modeled ventricles (phantoms) were developed. Jan D'hooge and colleagues from the University of Leuven generated cine loops mimicking normal, hypertrophied, and dysfunctional ventricles (**Figures 1**–**3**), and provided them to the vendors: after several attempts, results were similar for the principal vendors.

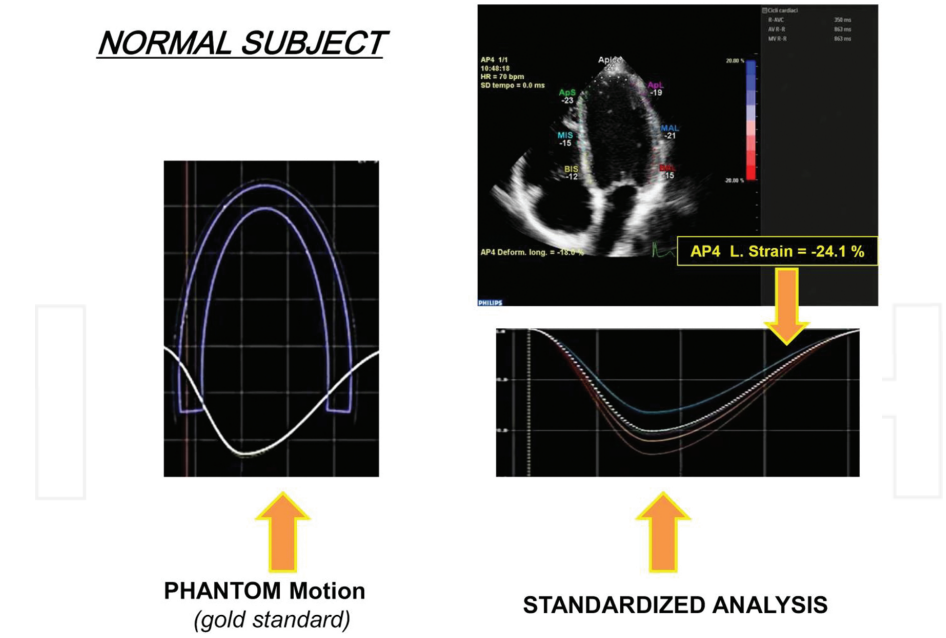

Figure 1. Global longitudinal strain calculation from phantom model (normal). AP4: apical four-chamber view; L. Strain: longitudinal strain.

http://dx.doi.org/10.5772/64261

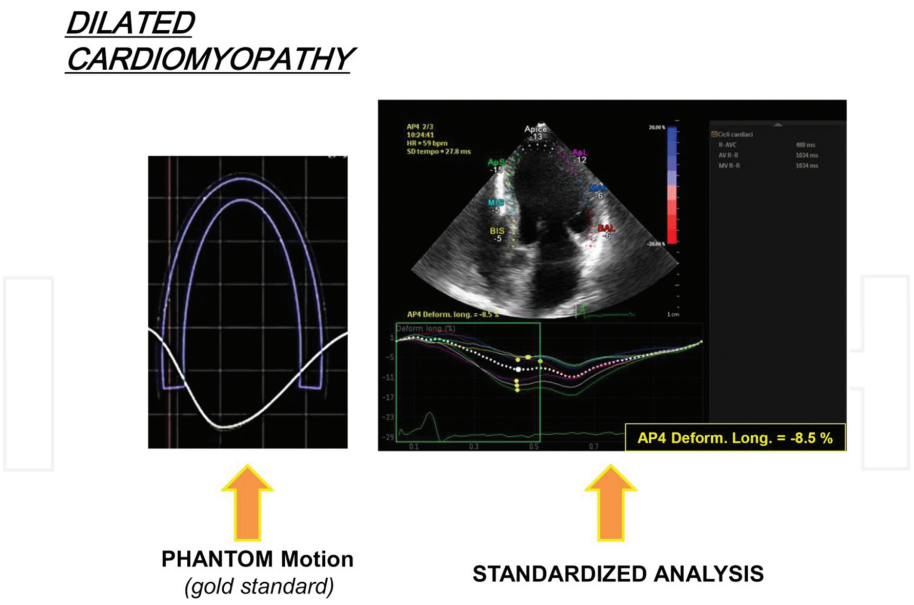

Figure 2. Global longitudinal strain from phantom model (dilated cardiomyopathy). AP4: apical four-chamber view; Deform. Long.: longitudinal deformation.

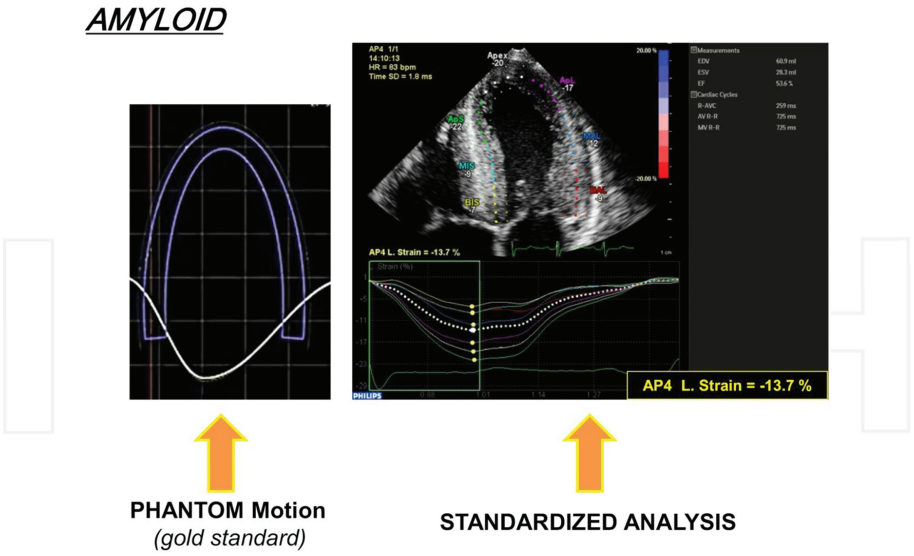

Figure 3. Global longitudinal strain from phantom model (amyloid). AP4: apical four-chamber view; L. Strain: longitudinal strain.

Moreover, a great effort has been made to standardize, speedup, and automatize (less subjective approach) GLS calculation, in order to offer immediate results to clinicians (bedside) and avoid errors in calculations (heart rate variability).

2.7. Clinical applications

2D STI has a wide field of clinical applications. We focus on main and novel fields of application (see also '**Table 4**') [38–48].

Field of Application	Explanation
Myocardial ischemia	Reduction in strain by 2D STI more objective than WMSI. Longitudinal, radial, and circumferential strain reduction in ischemia.
Myocardial infarction	Differentiation of transmural from subendocardial infarction. Remodeling.
Myocardial viability	Objective evaluation during stress echo. Differentiation of active contraction from passive tethering.
Heart failure with normal LVEF (HFnEF)	Twisting/untwisting.
Cardiac resynchronization therapy (CRT)	Longitudinal strain from TDI velocity with 2D STI radial strain. Longitudinal strain delay index. Radial strain and survival.
Takotsubo cardiomyopathy	Impaired longitudinal strain.
Restrictive cardiomyopathy	Impaired longitudinal deformation and twist.
Constrictive pericarditis	Impaired LV circumferential deformation and torsion.
Cardiotoxicity	Chemotherapy.
Detection of subclinical myocardial disease	Systemic hypertension, diabetes mellitus, systemic sclerosis, amyloidosis, and Duchenne's muscular dystrophy.
Valvular heart disease	Decreased radial, circumferential, and longitudinal strain in patients with severe aortic stenosis despite normal EF. Septal strain and mitral regurgitation.
Congenital heart disease	Right ventricular longitudinal strain and strain rate.

2D, bi-dimensional; 3D, three-dimensional; EF, ejection fraction; HFnEF, heart failure with normal ejection fraction; LV, left ventricle; STI, speckle-tracking imaging; TDI, tissue Doppler imaging; WMSI, wall motion score index.

Table 4. Principal clinical applications of speckle-tracking echocardiography.

Moreover, a recent meta-analysis presented the incremental value respective to EF retained by GLS [49]. It is essential to understand that technology development has today made available a fast, objective (automatized), and standardized definition of GLS, with final representation of bull's-eye plot of longitudinal strain value making it appealing, easily recognizable, and aligned with standardized segmentation of LV wall (**Figures 4** and **5**).

http://dx.doi.org/10.5772/64261

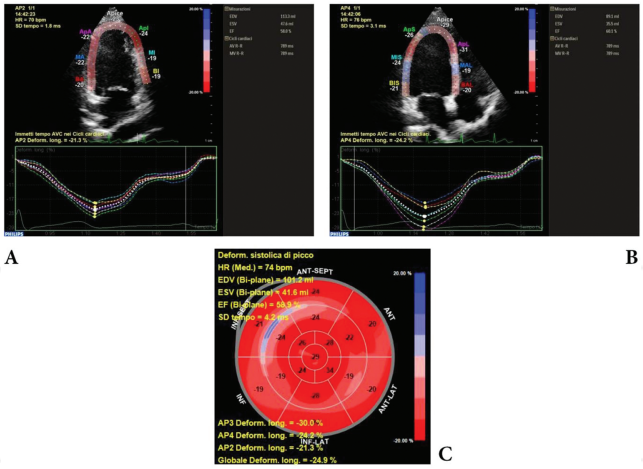

Figure 4. Global longitudinal strain calculation: on top showing tracking in four- (**B**) and two- (**A**) chamber view with strain curves; final bull's-eye plot (**C**) showing global results and superimposed regional values (Normal subject). AP2: apical two-chamber view; AP3: apical three-chamber view; AP4: apical four-chamber view; Deform. Long.: longitudinal deformation; EDV (bi-plane): end-diastolic volume (bi-plane); ESV (bi-plane): end-systolic volume (bi-plane); EF (bi-plane): ejection fraction (bi-plane); global Deform. Long. (GLS): global longitudinal strain; HR: heart rate.

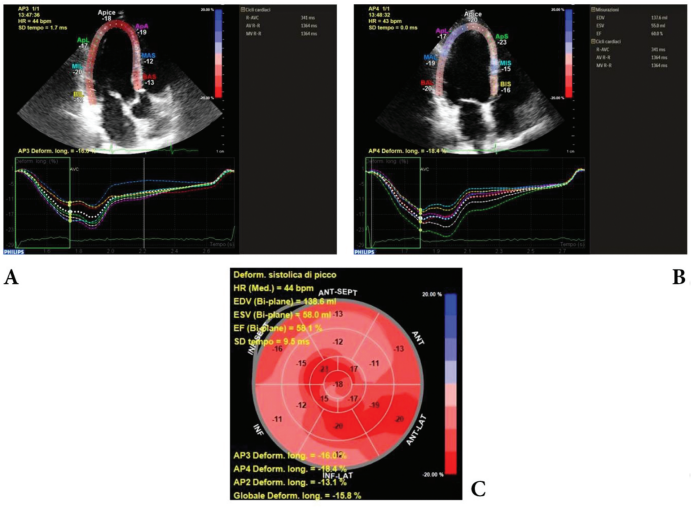

Figure 5. Global longitudinal strain calculation: on top showing tracking in three- (**A**) and four- (**B**) chamber view with strain curves; final bull's-eye plot (**C**) showing global results and superimposed regional values (dysfunctioning patient). AP2: apical two-chamber view; AP3: apical three-chamber view; AP4: apical four-chamber view; Deform. Long.: longitudinal deformation; EDV (bi-plane): end-diastolic volume (bi-plane); ESV (bi-plane): end-systolic volume (bi-plane); EF (bi-plane): ejection fraction (bi-plane); global Deform. Long. (GLS): global longitudinal strain; HR: heart rate.

2.7.1. Ischemic cardiomyopathy

In coronary artery disease, an assessment of myocardial ischemia other than simple visual wall motion score estimation (high inter-observer variability) has been invoked from a long time. Regional velocities (TDI) as well as peak systolic strain rate and systolic strain (TDI and STI) reduce linearly with a reduction in regional perfusion, time-delay prolongation to treatment, and the presence of fibrosis [14, 50, 51]. Subendocardial longitudinal fibers are the most vulnerable ones, resulting in an early deterioration of longitudinal strain, followed by radial and circumferential strains. Anyway, it's rather improper to consider a "radial function," because there are no myocardial fibers going in the radial direction. Actually, wall thickening measured by radial strain is a function of wall shortening, as the heart muscle is incompressible. At the same time, circumferential strain does not reflect circumferential fiber contraction because circumferential shortening is mainly due to the inward movement of mid-wall circumference as the wall thickens (inwards—as described by the eggshell model) [52–54]. Briefly, there would have been circumferential shortening even without circumferential fibers. These aspects, together with less standardized values than GLS, make GRS and GCS considerably reliable.

Dobutamine stress echocardiography is an important area of interest because in normal tissues an increased deformation occurs (continuously increasing strain/strain rate) as long as filling is not reduced by increased heart rate. On the contrary, acutely ischemic tissue during stress test shows less deformation and post-systolic deformation (PSD, thickening/shortening with radial/longitudinal strain, respectively), that is, the continued contraction of the myocardium after AVC. PSD is a common finding in myocardial ischemia. All these alterations are proportional to the severity of ischemia and persist in the experimental setting for up to 2 h after the ischemic insult resolution, with a peculiar time decay [55–57]. A noteworthy fact is that the stunned myocardium is characterized by decreased systolic deformation and PSD at rest, but almost normal systolic deformation and disappearance of PSD with dobutamine [50]. This behavior could be secondary to the heterogeneous contractile properties of the myocardium, probably linked to myofibrillar edema reducing the effective force myocardium can develop [58]. Furthermore, interstitial myocardial edema results in a sudden and temporary increase in end-diastolic wall thickness (this behavior is observed also in infarcted segments at the moment of reperfusion) [59, 60]. In chronic infarction, dobutamine is associated with low or no deformation increase, depending on the fibrosis extension (from subendocardial to transmurality involvement) [50].

2.7.2. Volume overload

Deformation is also closely related to ventricular geometry. Dilation is the end stage of most of the cardiomyopathies and heart valve diseases because for a given volume, the object with the smallest surface area is the sphere. This means that the same deformation (determined by the contractile force) can generate a larger stroke volume in a dilated heart. Similarly, in a dilated heart the same amount of stroke volume can be generated with less contractility and less deformation, that we can directly evaluate with strain(-rate) [14]. Remodeling in the long term will lead to irreversible damage to the heart muscle and finally ventricular dysfunction,

http://dx.doi.org/10.5772/64261

but there is no specific diagnostic method to detect subclinical changes in systolic function. STI and TDI might potentially be useful in detecting subclinical changes in cardiac function [60].

Mitral regurgitation (MR) is a typical volume overload condition. Primary MR leads to cardiac remodeling, increased left ventricular filling pressure, pulmonary arterial hypertension, and myocardial dysfunction. Conventional 2D, M-mode, and Doppler examination play a critical role in the initial and longitudinal assessment; anyway, most variables are load dependent and both afterload and preload are altered during the disease course. TDI and STI provide new parameters to assess regional and global myocardial performance and may help in identifying asymptomatic patients and choosing the optimal time for surgical correction. It is worthy to note that patients with severe primary degenerative MR may have near-normal left ventricle ejection fractions (LVEFs) because of disproportionately higher compensation in GLS. Moreover, the higher the GLS, the higher the risk of substantial reduction in LVEF (>10%) during the immediate postoperative period [61]. On the contrary, in patients tested at 6 months after surgery, when LV reverse remodeling has already settled, LVEF reductions >10% were associated with lower baseline strains [62]. Chronic ischemic MR instead is not a valvular disease per se but is rather a "ventricular disease." In particular, inferior MI has been recognized as the most frequent cause of ischemic MR because of the geometric distortion in the papillary muscle-bearing segments [63]. Therefore, the site of MI might be a more important determinant of MR degree in LV dysfunction than the extent of post-MI LV remodeling. Under normal conditions, the basal rotation, which is determined mainly by inferior and posterior myocardial segments [64], shortens the distance between the mitral valve and the head of the papillary muscles, contributing to MVC and counterbalancing the tethering forces. When local remodeling occurs, as in patients with inferior-posterior MIs, the basal strain and basal rotation are significantly lower and fail to shorten the distance between the papillary muscles and the mitral valve. Interestingly, Zito et al. demonstrated that basal rotation but not basal strain was an independent predictor of the severity of MR [65].

2.7.3. Pressure overload

Considering pressure overload pathology, aortic stenosis (AS) is the most common valve lesion causing chronic pressure overload on the LV. The development of symptoms in AS heralds a malignant phase of the condition and prompt aortic valve replacement results in a clear reduction in mortality [66]. In contrast, the management of patients with severe AS in the absence of symptoms remains one of the most controversial and debated areas in modern cardiology [67, 68].

The increased afterload leads to left ventricular hypertrophy and the basal septal is the first to show changes, due to increased wall stress according to the Laplace law [69]. It first shows a decrease in strain(-rate) and the development of PSD is observed, as well as the development of localized hypertrophy (septal bulge) [70]. Recently, GLS has been shown to be an independent predictor of outcomes in patients with severe asymptomatic AS, incremental to other echocardiographic markers [71]. Not to forget, the role of exercise testing in asymptomatic AS is well established, and recommended by guidelines in equivocal cases [72].

2.7.4. Mechanical dyssynchrony

Searching for the presence of mechanical dyssynchrony to identify potentially recruitable function, rather than looking only for electrocardiogram (ECG) manifestations of ventricular conduction delay, could increase the rate of cardiac resynchronization therapy (CRT) responders [73]. Mitigation of intraventricular dyssynchrony is currently thought to be the primary mechanism of improved myocardial performance with CRT. Anyway, many patients eligible for CRT have dilated ventricles with complex motion, especially if infarcted areas are present. Moreover, in dilated hearts local motion is importantly influenced by other myocardial segments and even by right ventricular motion [74]. That's why to this day, M-mode, 2D e TDI analyses have expressed modest sensitivity and specificity in measuring dyssynchrony and improving patient selection for CRT [73].

STI-based methods, mostly assessing the time difference between maximal values form different myocardial segments (e.g. septal to posterior wall motion delay [75], septal rebound stretch [76], wasted work ratio) [77, 78], are promising, but they must be validated in multicenter randomized trials.

2.7.5. Diabetic cardiomyopathy

Another field of interest is represented by diabetes mellitus because studies showed that myocardial damage occurred in at least 30% diabetic patients when LV diameter and LVEF were normal [79]. Diabetic myocardial diastolic dysfunction seems to precede systolic dysfunction, but this might be explained by the insensitivity of techniques for detecting LV systolic function. In many but small studies, longitudinal dysfunction (segmental GLS) occurred in early stages of diabetes, while LV torsion increased compensatively [80–84].

2.7.6. Cancer therapeutics-related cardiac dysfunction

Cardiotoxicity from cancer therapy has become a leading cause of morbidity and mortality in survivors [85, 86]. A careful consideration of potential cardiotoxicity during therapy and a focus on early detection and intervention are developing. Echocardiography is the cornerstone in the cardiac imaging evaluation of patients in preparation for, during, and after cancer therapy because of its wide availability, repeatability, versatility, lack of radiation exposure, and safety. The most commonly used parameter for monitoring LV function with echocardiography is LVEF. In addition, the calculation of LVEF should be combined with assessment of the wall motion score index [87]. Anyway, 2D echocardiography appears to be reliable in the detection of differences close to 10% in LVEF [88]. Because this is the same magnitude of change used to adjudicate cancer therapeutics-related cardiac dysfunction, the sensitivity of LVEF has been questioned. Moreover, detecting a decreased LVEF after anthracyclines may be too late for treatment [89], suggesting that more sensitive parameters of LV dysfunction could be helpful. The prognostic value of early measurement of systolic deformation indices (above all ΔGLS) measured in the prediction of subsequent LV systolic function has been evaluated in several studies, both in animals [90] and in humans [91–94].

http://dx.doi.org/10.5772/64261

2.7.7. Left atrium

Speckle tracking was recently applied to study the myocardial mechanics of a thin-walled structure such as the LA [95–98]. For the analysis, apical views are obtained using conventional 2D gray-scale echocardiography, during a breath-hold, with a stable electrocardiographic recording. The frame rate is set between 60 and 80 frames/s, and recordings are processed using acoustic-tracking software. The LA mechanical indices are calculated by averaging values observed in all LA segments (global strain) with a 15-segment or a 12-segment model. The software generates longitudinal strain and strain rate curves for each atrial segment. The radial deformation cannot be calculated because the LA wall is thin and the spatial resolution is limited [99].

2.7.8. Right ventricle

A recent methodological study has reported the feasibility, the reference values, and the reproducibility of right ventricular longitudinal strain measured by STI in normal patients and in patients with RV dysfunction [100]. The technique is similar as for LV: global strain is the average of six single segments (ROI) traced semi-automatically and processed by software packages (today, a dedicated software for RV does not exist). The evaluation of right ventricular function with STI, considering the important limitations of other parameters and methods, could offer more detailed information about regional and global RV mechanics with important clinical implications for non-invasive evaluation of RV systolic function (subclinical RV dysfunction). Further prospective studies are necessary to define its role in the management of patients.

3. Limitations

Rotation, deformation, and out-of-plane motion can cause speckle patterns to change between acquisitions (decorrelation). Loss of tracking can be limited acquiring at a proper frame rate. Image artifacts should be avoided. In general, high-quality acquisition is a prerequisite for optimal speckle-tracking results [16].

Among limitations of the method, we should include:

- Lack of reproducibility: even if much less compared with TDI, every STI study should include an intra- and interobserver variability testing [101];
- Intervendor variability: lack of standardization results in changes in reference values [102];
- Oversimplification due to software processing algorithms: automatic tracking of epicardial border (assumption of uniform thickness of myocardium); averaging of parameters within a segment; drifting;
- 2D imaging limitations: image quality; artifacts; image dropout; frame rate (low frame: no tracking, as at high heart frequencies; high frame: limited lateral resolution); lateral resolu-

tion and depth; depth dependence of transverse tracking; out-of-plane motion in short axis limiting tracking of the same ROI; noise.

Evaluation of radial strain poses important technical challenges compared to longitudinal one.

This is due to:

- Measurements in the axial plane are more reliable than those that depend on lateral and elevation (or azimuthal) resolution;
- Limited amount of tissue to track in the short-axis view of the non-hypertrophied heart;
- Placement of the ROI is user defined;
- Intervendors' differences.

4. Conclusions

Speckle tracking is actually a reality in echocardiography. Simple protocols of acquisition and novel processing packages have made available deformation analysis in daily clinical arena.

Overcoming many of the previous limitations, thanks to technological development, including 3D introduction and STI, offers to the cardiologists the potential benefit of a solid, fast, easy, and reproducible quantization of myocardial mechanics [37].

Author details

Iacopo Fabiani[1*], Nicola Riccardo Pugliese[2], Veronica Santini[1], Lorenzo Conte[1] and Vitantonio Di Bello[1]

*Address all correspondence to: iacopofabiani@gmail.com

1 Dept. Section Universitary Cardio-Angiology, Surgical, Medical, Molecular and Critical Area Pathology Department, Pisa Univeristy, Pisa, Italy

2 Operative Unit Cardio-Vascular Disease Univ., Surgical, Medical, Molecular and Critical Area Pathology Department, Pisa Univeristy, Pisa, Italy

References

[1] Perk G, Tunick PA, Kronzon I. Non-Doppler two-dimensional strain imaging by echocardiography – from technical considerations to clinical applications. J Am Soc Echocardiogr. 2007;20:234–243. DOI: 10.1016/j.echo.2006.08.023

[2] Dandel M, Lehmkuhl H, Knosalla C, Suramelashvili N, Hetzer R. Strain and strain rate imaging by echocardiography – basic concepts and clinical applicability. Curr Cardiol Rev. 2009;5:133–148. DOI: 10.2174/157340309788166642

[3] Blessberger H, Binder T. NON-invasive imaging: two dimensional speckle tracking echocardiography: basic principles. Heart. 2010;96:716–722. DOI: 10.1136/hrt.2007.141002

[4] Blessberger H, Binder T. Two dimensional speckle tracking echocardiography: clinical applications. Heart. 2010;96:2032–2040. DOI: 10.1136/hrt.2010.199885

[5] Storaa C, Aberg P, Lind B, Brodin LA. Effect of angular error on tissue Doppler velocities and strain. Echocardiography. 2003;20:581–587. DOI: 10.1046/j.1540-8175.2003.01135

[6] Dandel M, Hetzer R. Echocardiographic strain and strain rate imaging – clinical applications. Int J Cardiol. 2009;132:11–24. DOI: 10.1016/j.ijcard.2008.06.091

[7] Dokainish H, Sengupta R, Pillai M, Bobek J, Lakkis N. Usefulness of new diastolic strain and strain rate indexes for the estimation of left ventricular filling pressure. Am J Cardiol. 2008;101:1504–1509. DOI: 10.1016/j.amjcard.2008.01.037

[8] Gorcsan J, 3rd, Tanaka H. Echocardiographic assessment of myocardial strain. J Am Coll Cardiol. 2011;58:1401–1413. DOI: 10.1016/j.jacc.2011.06.038

[9] Mor-Avi V, Lang RM, Badano LP, Belohlavek M, Cardim NM, Derumeaux G, et al. Current and evolving echocardiographic techniques for the quantitative evaluation of cardiac mechanics: ASE/EAE consensus statement on methodology and indications endorsed by the Japanese Society of Echocardiography. Euro J Echocardiogr. 2011;12:167–205. DOI: 10.1093/ejechocard/jer021

[10] Streeter DD, Jr., Spotnitz HM, Patel DP, Ross J, Jr., Sonnenblick EH. Fiber orientation in the canine left ventricle during diastole and systole. Circ Res. 1969;24:339–347. DOI: 10.1371/journal.pone.0132360

[11] Greenbaum RA, Ho SY, Gibson DG, Becker AE, Anderson RH. Left ventricular fibre architecture in man. Br Heart J. 1981;45:248–263. DOI: 10.1136/hrt.45.3.248

[12] Torrent-Guasp F, Buckberg GD, Clemente C, Cox JL, Coghlan HC, Gharib M. The structure and function of the helical heart and its buttress wrapping. I. The normal macroscopic structure of the heart. Semin Thorac Cardiovasc Surg. 2001;13:301–319. DOI: none

[13] Sun JP. Ventricular Torsion. In: Marwick TH, Yu CM, Sun JP. Myocardial Imaging Tissue Doppler and Speckle Tracking. Wiley-Blackwell; Hoboken, New Jersey, 2007. pp. 273–277. DOI: 10.1002/9780470692448.ch23

[14] Bijnens BH, Cikes M, Claus P, Sutherland GR. Velocity and deformation imaging for the assessment of myocardial dysfunction. Eur J Echocardiogr. 2009;10:216–226. DOI: 10.1093/ejechocard/jen323

[15] Heimdal A. Technical Principles of Tissue Velocity and Strain Imaging Methods. In: Marwick TH, Yu CM, Sun JP. Myocardial Imaging Tissue Doppler and Speckle Tracking. Wiley-Blackwell; Hoboken, New Jersey, 2007. pp. 3–16. DOI: 10.1002/9780470692448.ch1

[16] D'hooge J. Principles and Different Techniques for Speckle Tracking. In: Marwick TH, Yu CM, Sun JP. Myocardial Imaging Tissue Doppler and Speckle Tracking. Wiley-Blackwell; Hoboken, New Jersey, 2007. pp. 17–25. DOI: 10.1002/9780470692448.ch2

[17] Vannan MA, Pedrizzetti G, Li P, Gurudevan S, Houle H, Main J, et al. Effect of cardiac resynchronization therapy on longitudinal and circumferential left ventricular mechanics by velocity vector imaging: description and initial clinical application of a novel method using high-frame rate B-mode echocardiographic images. Echocardiography. 2005;22:826–830. DOI: 10.1111/j.1540-8175.2005.00172.x

[18] Biswas M, Sudhakar S, Nanda NC, Buckberg G, Pradhan M, Roomi AU, Gorissen W, Houle H. Two- and three-dimensional speckle tracking echocardiography: clinical aplications and future directions. Echocardiography. 2013;30:88–105. DOI: 10.1111/echo.12079

[19] Voigt JU, Pedrizzetti G, Lysyansky P, Marwick TH, Houle H, Baumann R et al. Definitions for a common standard for 2D speckle tracking echocardiography: consensus document of the EACVI/ASE/industry task force to standardize deformation imaging. J Am Soc Echocardiogr. 2015;28(2):183–193. DOI: 10.1016/j.echo.2014.11.003

[20] Hurlburt HM, Aurigemma GP, Hill JC, Narayanan A, Gaasch WH, Vinch CS, et al. Direct ultrasound measurement of longitudinal, circumferential, and radial strain using 2-dimensional strain imaging in normal adults. Echocardiography. 2007;24:723–731. DOI: 10.1111/j.1540-8175.2007.00460.x

[21] Yingchoncharoen T, Agarwal S, Popovic ZB, Marwick TH. Normal ranges of left ventricular strain: a meta-analysis. J Am Soc Echocardiogr. 2013;26:185–191. DOI: 10.1016/j.echo.2012.10.008

[22] Nguyen JS, Lakkis NM, Bobek J, Goswami R, Dokainish H. Systolic and diastolic myocardial mechanics in patients with cardiac disease and preserved ejection fraction: impact of left ventricular filling pressure. J Am Soc Echocardiogr. 2010;23:1273–1280. DOI: 10.1016/j.echo.2010.09.008

[23] Amundsen BH, Helle-Valle T, Edvardsen T, Torp H, Crosby J, Lyseggen E, et al. Noninvasive myocardial strain measurement by speckle tracking echocardiography: validation against sonomicrometry and tagged magnetic resonance imaging. J Am Coll Cardiol. 2006;47:789–793. DOI: 10.1016/j.jacc.2005.10.040

[24] Cho GY, Chan J, Leano R, Strudwick M, Marwick TH. Comparison of two-dimensional speckle and tissue velocity based strain and validation with harmonic phase magnetic resonance imaging. Am J Cardiol. 2006;97:1661–1666. DOI: 10.1016/j.amjcard.2005.12.063

[25] Papademetris X, Sinusas AJ, Dione DP, Duncan JS. Estimation of 3D left ventricular deformation from echocardiography. Med Image Anal. 2001;5:17–28. DOI: 10.1016/S1361-8415(00)00022-0

[26] Elen A, Choi HF, Loeckx D, Gao H, Claus P, Suetens P, et al. Three-dimensional cardiac strain estimation using spatio-temporal elastic registration of ultrasound images: a feasibility study. IEEE Trans Med Imaging. 2008;27:1580–1591. DOI: 10.1109/TMI.2008.2004420

[27] Crosby J, Amundsen BH, Hergum T, Remme EW, Langeland S, Torp H. 3-D speckle tracking for assessment of regional left ventricular function. Ultrasound Med Biol. 2009;35:458–471. DOI: 10.1016/j.ultrasmedbio.2008.09.011

[28] Hayat D, Kloeckner M, Nahum J, Ecochard-Dugelay E, Dubois-Rande JL, Jean-Francois D, et al. Comparison of real-time three-dimensional speckle tracking to magnetic resonance imaging in patients with coronary heart disease. Am J Cardiol. 2012;109:180–186. DOI: 10.1016/j.amjcard.2011.08.030

[29] Abate E, Hoogslag GE, Antoni ML, Nucifora G, Delgado V, Holman ER, et al. Value of three-dimensional speckle-tracking longitudinal strain for predicting improvement of left ventricular function after acute myocardial infarction. Am J Cardiol. 2012;110:961–967. DOI: 10.1016/j.amjcard.2012.05.023

[30] Kleijn SA, Aly MF, Terwee CB, van Rossum AC, Kamp O. Three-dimensional speckle tracking echocardiography for automatic assessment of global and regional left ventricular function based on area strain. J Am Soc Echocardiogr. 2011;24:314–321. DOI: 10.1016/j.echo.2011.01.014

[31] Kleijn SA, Aly MF, Knol DL, Terwee CB, Jansma EP, Abd El-Hady YA, et al. A meta-analysis of left ventricular dyssynchrony assessment and prediction of response to cardiac resynchronization therapy by three-dimensional echocardiography. Eur Heart J Cardiovasc Imaging. 2012;13:763–775. DOI: 10.1093/ehjci/jes041

[32] Yodwut C, Weinert L, Klas B, Lang RM, Mor-Avi V. Effects of frame rate on three-dimensional speckle-tracking-based measurements of myocardial deformation. J Am Soc Echocardiogr. 2012;25:978–985. DOI: 10.1016/j.echo.2012.06.001

[33] Urbano-Moral JA, Patel AR, Maron MS, Arias-Godinez JA, Pandian NG. Three-dimensional speckle-tracking echocardiography: methodological aspects and clinical potential. Echocardiography. 2012;29:997–1010. DOI: 10.1111/j.1540-8175.2012.01773.x

[34] Urbano-Moral JA, Rowin EJ, Maron MS, Crean A, Pandian NG. Investigation of global and regional myocardial mechanics with 3-dimensional speckle tracking echocardiography and relations to hypertrophy and fibrosis in hypertrophic cardiomyopathy. Circ Cardiovasc Imaging. 2014;7:11–19. DOI: 10.1161/CIRCIMAGING.113.000842

[35] Perez de Isla L, Millan M, Lennie V, Quezada M, Guinea J, Macaya C, et al. Area strain: normal values for a new parameter in healthy people. Rev Esp Cardiol. 2011;64:1194–1197. DOI: 10.1016/j.recesp.2011.03.021

[36] Thomas JD, Badano LP. EACVI-ASE-industry initiative to standardize deformation imaging: a brief update from the co-chairs. Eur Heart J Cardiovasc Imaging. 2013;14:1039–1040. DOI: 10.1093/ehjci/jet184

[37] Voigt JU, Pedrizzetti G, Lysyansky P, Marwick TH, Houle H, Baumann R, et al. Definitions for a common standard for 2D speckle tracking echocardiography: consensus document of the EACVI/ASE/Industry Task Force to standardize deformation imaging. Eur Heart J Cardiovasc Imaging. 2015;16:1–11. DOI: 10.1093/ehjci/jeu184

[38] Heggemann F, Weiss C, Hamm K, Kaden J, Suselbeck T, Papavassiliu T, et al. Global and regional myocardial function quantification by two-dimensional strain in Takotsubo cardiomyopathy. Eur J Echocardiogr. 2009;10:760–764. DOI: 10.1093/ejechocard/jep062

[39] Shimoni S, Gendelman G, Ayzenberg O, Smirin N, Lysyansky P, Edri O, et al. Differential effects of coronary artery stenosis on myocardial function: the value of myocardial strain analysis for the detection of coronary artery disease. J Am Soc Echocardiogr. 2011;24:748–757. DOI: 10.1016/j.echo.2011.03.007

[40] Becker M, Hoffmann R, Kuhl HP, Grawe H, Katoh M, Kramann R, et al. Analysis of myocardial deformation based on ultrasonic pixel tracking to determine transmurality in chronic myocardial infarction. Eur Heart J. 006;27:2560–2566. DOI: 10.1093/eurheartj/ehl288

[41] Chan J, Hanekom L, Wong C, Leano R, Cho GY, Marwick TH. Differentiation of subendocardial and transmural infarction using two-dimensional strain rate imaging to assess short-axis and long-axis myocardial function. J Am Coll Cardiol. 2006;48:2026–2033. DOI: 10.1016/j.jacc.2006.07.050

[42] Tan YT, Wenzelburger F, Lee E, Heatlie G, Leyva F, Patel K, et al. The pathophysiology of heart failure with normal ejection fraction: exercise echocardiography reveals complex abnormalities of both systolic and diastolic ventricular function involving torsion, untwist, and longitudinal motion. J Am Coll Cardiol. 2009;54:36–46. DOI: 10.1016/j.jacc.2009.03.037

[43] Gorcsan J, 3rd, Tanabe M, Bleeker GB, Suffoletto MS, Thomas NC, Saba S, et al. Combined longitudinal and radial dyssynchrony predicts ventricular response after resynchronization therapy. J Am Coll Cardiol. 2007;50:1476–1483. DOI: 10.1016/j.jacc.2007.06.043

[44] Delgado V, van Bommel RJ, Bertini M, Borleffs CJ, Marsan NA, Arnold CT, et al. Relative merits of left ventricular dyssynchrony, left ventricular lead position, and myocardial scar to predict long-term survival of ischemic heart failure patients undergoing cardiac

resynchronization therapy. Circulation. 2011;123:70–78. DOI: 10.1161/CIRCULATIONAHA.110.945345

[45] Bellavia D, Abraham TP, Pellikka PA, Al-Zahrani GB, Dispenzieri A, Oh JK, et al. Detection of left ventricular systolic dysfunction in cardiac amyloidosis with strain rate echocardiography. J Am Soc Echocardiogr. 2007;20:1194–1202. DOI: 10.1016/j.echo.2007.02.025

[46] Delgado V, Tops LF, van Bommel RJ, van der Kley F, Marsan NA, Klautz RJ, et al. Strain analysis in patients with severe aortic stenosis and preserved left ventricular ejection fraction undergoing surgical valve replacement. Eur Heart J. 2009;30:3037–3047. DOI: 10.1093/eurheartj/ehp351

[47] De Isla LP, De Agustin A, Rodrigo JL, Almeria C, del Carmen Manzano M, Rodriguez E, et al. Chronic mitral regurgitation: a pilot study to assess preoperative left ventricular contractile function using speckle-tracking echocardiography. J Am Soc Echocardiogr. 2009;22:831–838. DOI: 10.1016/j.echo.2009.04.016

[48] Sengupta PP, Krishnamoorthy VK, Abhayaratna WP, Korinek J, Belohlavek M, Sundt TM, 3rd, et al. Disparate patterns of left ventricular mechanics differentiate constrictive pericarditis from restrictive cardiomyopathy. JACC Cardiovasc Imaging. 2008;1:29–38. DOI: 10.1016/j.jcmg.2007.10.006

[49] Kalam K, Otahal P, Marwick TH. Prognostic implications of global LV dysfunction: a systematic review and meta-analysis of global longitudinal strain and ejection fraction. Heart. 2014;100:1673–1680. DOI: 10.1136/heartjnl-2014-305538

[50] Bijnens B, Claus P, Weidemann F, Strotmann J, Sutherland GR. Investigating cardiac function using motion and deformation analysis in the setting of coronary artery disease. Circulation. 2007;116:2453–2464. DOI: 10.1161/CIRCULATIONAHA.106.684357

[51] Turschner O, D'Hooge J, Dommke C, Claus P, Verbeken E, De Scheerder I, et al. The sequential changes in myocardial thickness and thickening which occur during acute transmural infarction, infarct reperfusion and the resultant expression of reperfusion injury. Eur Heart J. 2004;25:794–803. DOI: 10.1016/j.ehj.2004.01.006

[52] Carlhall CJ, Lindstrom L, Wranne B, Nylander E. Atrioventricular plane displacement correlates closely to circulatory dimensions but not to ejection fraction in normal young subjects. Clin Physiol. 2001;21:621–628. DOI: 10.1046/j.1365-2281.2001.00356.x

[53] Zaky A, Nasser WK, Feigenbaum H. A study of mitral valve action recorded by reflected ultrasound and its application in the diagnosis of mitral stenosis. Circulation. 1968;37:789–799. DOI: 10.1161/01.CIR.37.5.789

[54] Roberson DA, Cui W. Tissue Doppler imaging measurement of left ventricular systolic function in children: mitral annular displacement index is superior to peak velocity. J Am Soc Echocardiogr. 2009;22:376–382. DOI: 10.1016/j.echo.2009.01.008

[55] Voigt JU, Exner B, Schmiedehausen K, Huchzermeyer C, Reulbach U, Nixdorff U, et al. Strain-rate imaging during dobutamine stress echocardiography provides objective evidence of inducible ischemia. Circulation. 2003;107:2120–2126. DOI: 10.1161/01.CIR.0000065249.69988.AA

[56] Weidemann F, Dommke C, Bijnens B, Claus P, D'Hooge J, Mertens P, et al. Defining the transmurality of a chronic myocardial infarction by ultrasonic strain-rate imaging: implications for identifying intramural viability: an experimental study. Circulation. 2003;107:883–888. DOI: 10.1161/01.CIR.0000050146.66577.4B

[57] Asanuma T, Uranishi A, Masuda K, Ishikura F, Beppu S, Nakatani S. Assessment of myocardial ischemic memory using persistence of post-systolic thickening after recovery from ischemia. JACC Cardiovasc Imaging. 2009;2:1253–1261. DOI: 10.1016/j.jcmg.2009.07.008

[58] Bragadeesh T, Jayaweera AR, Pascotto M, Micari A, Le DE, Kramer CM, et al. Post-ischaemic myocardial dysfunction (stunning) results from myofibrillar oedema. Heart. 2008;94:166–171. DOI: 10.1136/hrt.2006.102434

[59] Merli E, Sutherland GR, Bijnens B, Fischer A, Chaparro M, Karu T, et al. Usefulness of changes in left ventricular wall thickness to predict full or partial pressure reperfusion in ST-elevation acute myocardial infarction. Am J Cardiol. 2008;102:249–256. DOI: 10.1016/j.amjcard.2008.03.047

[60] Marciniak A, Claus P, Sutherland GR, Marciniak M, Karu T, Baltabaeva A, et al. Changes in systolic left ventricular function in isolated mitral regurgitation. A strain rate imaging study. Eur Heart J. 2007;28:2627–2636. DOI: 10.1093/eurheartj/ehm072

[61] Pandis D, Sengupta PP, Castillo JG, Caracciolo G, Fischer GW, Narula J, et al. Assessment of longitudinal myocardial mechanics in patients with degenerative mitral valve regurgitation predicts postoperative worsening of left ventricular systolic function. J Am Soc Echocardiogr. 2014;27:627–638. DOI: 10.1016/j.echo.2014.02.008

[62] Florescu M, Benea DC, Rimbas RC, Cerin G, Diena M, Lanzzillo G, et al. Myocardial systolic velocities and deformation assessed by speckle tracking for early detection of left ventricular dysfunction in asymptomatic patients with severe primary mitral regurgitation. Echocardiography. 2012;29:326–333. DOI: 10.1111/j.1540-8175.2011.01563.x

[63] Kumanohoso T, Otsuji Y, Yoshifuku S, Matsukida K, Koriyama C, Kisanuki A, et al. Mechanism of higher incidence of ischemic mitral regurgitation in patients with inferior myocardial infarction: quantitative analysis of left ventricular and mitral valve geometry in 103 patients with prior myocardial infarction. J Thorac Cardiovasc Surg. 2003;125:135–143. DOI: 10.1067/mva.2003.78

[64] Gustafsson U, Lindqvist P, Morner S, Waldenstrom A. Assessment of regional rotation patterns improves the understanding of the systolic and diastolic left ventricular

function: an echocardiographic speckle-tracking study in healthy individuals. Eur J Echocardiogr. 2009;10:56–61. DOI: 10.1093/ejechocard/jen141

[65] Zito C, Cusma-Piccione M, Oreto L, Tripepi S, Mohammed M, Di Bella G, et al. In patients with post-infarction left ventricular dysfunction, how does impaired basal rotation affect chronic ischemic mitral regurgitation? J Am Soc Echocardiogr. 2013;26:1118–1129. DOI: 10.1016/j.echo.2013.04.017

[66] Singh A, Steadman CD, McCann GP. Advances in the understanding of the pathophysiology and management of aortic stenosis: role of novel imaging techniques. Can J Cardiol. 2014;30:994–1003. DOI: 10.1016/j.cjca.2014.03.008

[67] Shah PK. Should severe aortic stenosis be operated on before symptom onset? Severe aortic stenosis should not be operated on before symptom onset. Circulation. 2012;126:118–125. DOI: 10.1161/CIRCULATIONAHA.111.079368

[68] Carabello BA. Should severe aortic stenosis be operated on before symptom onset? Aortic valve replacement should be operated on before symptom onset. Circulation. 2012;126:112–117. DOI: 0.1161/CIRCULATIONAHA.111.079350

[69] Carabello BA. The relationship of left ventricular geometry and hypertrophy to left ventricular function in valvular heart disease. J Heart Valve Dis. 1995;4 Suppl 2:S132–138; discussion S138–139. DOI: none

[70] Baltabaeva A, Marciniak M, Bijnens B, Moggridge J, He FJ, Antonios TF, et al. Regional left ventricular deformation and geometry analysis provides insights in myocardial remodelling in mild to moderate hypertension. Eur J Echocardiogr. 2008;9:501–508. DOI: 10.1016/j.euje.2007.08.004

[71] Yingchoncharoen T, Gibby C, Rodriguez LL, Grimm RA, Marwick TH. Association of myocardial deformation with outcome in asymptomatic aortic stenosis with normal ejection fraction. Circ Cardiovasc Imaging. 2012;5:719–725. DOI: 10.1161/CIRCIMAGING.112.977348

[72] Nishimura RA, Otto CM, Bonow RO, Carabello BA, Erwin JP, 3rd, Guyton RA, et al. 2014 AHA/ACC guideline for the management of patients with valvular heart disease: executive summary: a report of the American College of Cardiology/American Heart Association Task Force on practice guidelines. Circulation. 2014;129:2440–2492. DOI: 10.1161/CIR.0000000000000029

[73] Hawkins NM, Petrie MC, Burgess MI, McMurray JJ. Selecting patients for cardiac resynchronization therapy: the fallacy of echocardiographic dyssynchrony. J Am Coll Cardiol. 2009;53:1944–1959. DOI: 10.1016/j.jacc.2008.11.062

[74] Marciniak M, Bijnens B, Baltabaeva A, Marciniak A, Parsai C, Claus P, et al. Interventricular interaction as a possible mechanism for the presence of a biphasic systolic velocity profile in normal left ventricular free walls. Heart. 2008;94:1058–1064. DOI: 10.1136/hrt.2007.126938

[75] Suffoletto MS, Dohi K, Cannesson M, Saba S, Gorcsan J, 3rd. Novel speckle-tracking radial strain from routine black-and-white echocardiographic images to quantify dyssynchrony and predict response to cardiac resynchronization therapy. Circulation. 2006;113:960–968. DOI: 10.1161/CIRCULATIONAHA.105.571455

[76] Carasso S, Rakowski H, Witte KK, Smith P, Carasso D, Garceau P, et al. Left ventricular strain patterns in dilated cardiomyopathy predict response to cardiac resynchronization therapy: timing is not everything. J Am Soc Echocardiogr. 2009;22:242–250. DOI: 10.1016/j.echo.2008.12.003

[77] Russell K, Eriksen M, Aaberge L, Wilhelmsen N, Skulstad H, Remme EW, et al. A novel clinical method for quantification of regional left ventricular pressure-strain loop area: a non-invasive index of myocardial work. Eur Heart J. 2012;33:724–733. DOI: 10.1093/eurheartj/ehs016

[78] Russell K, Eriksen M, Aaberge L, Wilhelmsen N, Skulstad H, Gjesdal O, et al. Assessment of wasted myocardial work: a novel method to quantify energy loss due to uncoordinated left ventricular contractions. Am J Physiol Heart Circ Physiol. 2013;305:H996–1003. DOI: 10.1152/ajpheart.00191.2013

[79] Galderisi M. Diastolic dysfunction and diabetic cardiomyopathy: evaluation by Doppler echocardiography. J Am Coll Cardiol. 2006;48:1548–1551. DOI: 10.1016/j.jacc.2006.07.033

[80] Guo R, Wang K, Song W, Cong T, Shang ZJ, Sun YH, et al. Myocardial dysfunction in early diabetes patients with microalbuminuria: a 2-dimensional speckle tracking strain study. Cell Biochem Biophys. 2014;70:573–578. DOI: 10.1007/s12013-014-9958-8

[81] Shim CY, Park S, Choi EY, Kang SM, Cha BS, Ha JW, et al. Is albuminuria an indicator of myocardial dysfunction in diabetic patients without overt heart disease? A study with Doppler strain and strain rate imaging. Metabolism. 2008;57:448–452. DOI: 10.1016/j.metabol.2007.11.003

[82] Ernande L, Rietzschel ER, Bergerot C, De Buyzere ML, Schnell F, Groisne L, et al. Impaired myocardial radial function in asymptomatic patients with type 2 diabetes mellitus: a speckle-tracking imaging study. J Am Soc Echocardiogr. 2010;23:1266–1272. DOI: 10.1016/j.echo.2010.09.007

[83] Ernande L, Bergerot C, Rietzschel ER, De Buyzere ML, Thibault H, Pignonblanc PG, et al. Diastolic dysfunction in patients with type 2 diabetes mellitus: is it really the first marker of diabetic cardiomyopathy? J Am Soc Echocardiogr. 2011;24:1268–1275 e1261. DOI: 10.1016/j.echo.2011.07.017

[84] Karagoz A, Bezgin T, Kutluturk I, Kulahcioglu S, Tanboga IH, Guler A, et al. Subclinical left ventricular systolic dysfunction in diabetic patients and its association with retinopathy: a 2D speckle tracking echocardiography study. Herz. 2014. DOI: 10.1007/s00059-014-4138-6

[85] Hooning MJ, Botma A, Aleman BM, Baaijens MH, Bartelink H, Klijn JG, et al. Long-term risk of cardiovascular disease in 10-year survivors of breast cancer. J Natl Cancer Inst. 2007;99:365–375. DOI: 10.1093/jnci/djk064

[86] Doyle JJ, Neugut AI, Jacobson JS, Grann VR, Hershman DL. Chemotherapy and cardiotoxicity in older breast cancer patients: a population-based study. J Clin Oncol. 2005;23:8597–8605. DOI: 10.1200/JCO.2005.02.5841

[87] Lang RM, Bierig M, Devereux RB, Flachskampf FA, Foster E, Pellikka PA, et al. Recommendations for chamber quantification: a report from the American Society of Echocardiography's Guidelines and Standards Committee and the Chamber Quantification Writing Group, developed in conjunction with the European Association of Echocardiography, a branch of the European Society of Cardiology. J Am Soc Echocardiogr. 2005;18:1440–1463. DOI: 10.1016/j.echo.2005.10.005

[88] Thavendiranathan P, Grant AD, Negishi T, Plana JC, Popovic ZB, Marwick TH. Reproducibility of echocardiographic techniques for sequential assessment of left ventricular ejection fraction and volumes: application to patients undergoing cancer chemotherapy. J Am Coll Cardiol. 2013;61:77–84. DOI: 10.1016/j.jacc.2012.09.035

[89] Cardinale D, Colombo A, Lamantia G, Colombo N, Civelli M, De Giacomi G, et al. Anthracycline-induced cardiomyopathy: clinical relevance and response to pharmacologic therapy. J Am Coll Cardiol. 2010;55:213–220. DOI: 10.1016/j.jacc.2009.03.095

[90] Neilan TG, Jassal DS, Perez-Sanz TM, Raher MJ, Pradhan AD, Buys ES, et al. Tissue Doppler imaging predicts left ventricular dysfunction and mortality in a murine model of cardiac injury. Eur Heart J. 2006;27:1868–1875. DOI: 10.1093/eurheartj/ehl013

[91] Sawaya H, Sebag IA, Plana JC, Januzzi JL, Ky B, Cohen V, et al. Early detection and prediction of cardiotoxicity in chemotherapy-treated patients. Am J Cardiol. 2011;107:1375–1380. DOI: 10.1016/j.amjcard.2011.01.006

[92] Fallah-Rad N, Walker JR, Wassef A, Lytwyn M, Bohonis S, Fang T, et al. The utility of cardiac biomarkers, tissue velocity and strain imaging, and cardiac magnetic resonance imaging in predicting early left ventricular dysfunction in patients with human epidermal growth factor receptor II-positive breast cancer treated with adjuvant trastuzumab therapy. J Am Coll Cardiol. 2011;57:2263–2270. DOI: 10.1016/j.jacc.2010.11.063

[93] Poterucha JT, Kutty S, Lindquist RK, Li L, Eidem BW. Changes in left ventricular longitudinal strain with anthracycline chemotherapy in adolescents precede subsequent decreased left ventricular ejection fraction. J Am Soc Echocardiogr. 2012;25:733–740. DOI: 10.1016/j.echo.2012.04.007

[94] Sawaya H, Sebag IA, Plana JC, Januzzi JL, Ky B, Tan TC, et al. Assessment of echocardiography and biomarkers for the extended prediction of cardiotoxicity in patients treated with anthracyclines, taxanes, and trastuzumab. Circ Cardiovasc Imaging. 2012;5:596–603. DOI: 10.1161/CIRCIMAGING.112.973321

[95] Sirbu C, Herbots L, D'Hooge J, Claus P, Marciniak A, Langeland T, et al. Feasibility of strain and strain rate imaging for the assessment of regional left atrial deformation: a study in normal subjects. Eur J Echocardiogr. 2006;7:199–208. DOI: 10.1016/j.euje.2005.06.001

[96] Cameli M, Lisi M, Focardi M, Reccia R, Natali BM, Sparla S, et al. Left atrial deformation analysis by speckle tracking echocardiography for prediction of cardiovascular outcomes. Am J Cardiol. 2012;110:264–269. DOI: 10.1016/j.amjcard.2012.03.022

[97] Vianna-Pinton R, Moreno CA, Baxter CM, Lee KS, Tsang TS, Appleton CP. Two-dimensional speckle-tracking echocardiography of the left atrium: feasibility and regional contraction and relaxation differences in normal subjects. J Am Soc Echocardiogr. 2009;22:299–305. DOI: 10.1016/j.echo.2008.12.017

[98] Okamatsu K, Takeuchi M, Nakai H, Nishikage T, Salgo IS, Husson S, et al. Effects of aging on left atrial function assessed by two-dimensional speckle tracking echocardiography. J Am Soc Echocardiogr. 2009;22:70–75. DOI: 10.1016/j.echo.2008.11.006

[99] D'Hooge J, Heimdal A, Jamal F, Kukulski T, Bijnens B, Rademakers F, et al. Regional strain and strain rate measurements by cardiac ultrasound: principles, implementation and limitations. Eur J Echocardiogr. 2000;1:154–170. DOI: 10.1053/euje.2000.0031

[100] Meris A, Faletra F, Conca C, Klersy C, Regoli F, Klimusina J, et al. Timing and magnitude of regional right ventricular function: a speckle tracking-derived strain study of normal subjects and patients with right ventricular dysfunction. J Am Soc Echocardiogr. 2010;23:823–831. DOI: 10.1016/j.echo.2010.05.009

[101] Kleijn SA, Aly MF, Terwee CB, van Rossum AC, Kamp O. Reliability of left ventricular volumes and function measurements using three-dimensional speckle tracking echocardiography. Eur Heart J Cardiovasc Imaging. 2012;13:159–168. DOI: 10.1093/ejechocard/jer174

[102] Gayat E, Ahmad H, Weinert L, Lang RM, Mor-Avi V. Reproducibility and inter-vendor variability of left ventricular deformation measurements by three-dimensional speckle-tracking echocardiography. J Am Soc Echocardiogr. 2011;24:878–885. DOI: 10.1016/j.echo.2011.04.016